Int. J. Heat Mass Transfer. Vol. 29, No. 11, pp. 1711–1722, 1986
Printed in Great Britain

0017-9310/86 \$3.00+0.00
Pergamon Journals Ltd.

Laminar mixed convection in a partially blocked, vertical channel

S. HABCHI and S. ACHARYA
Mechanical Engineering Department, Louisiana State University, Baton Rouge, LA 70803, U.S.A.

(*Received* 9 *October* 1985 *and in final form* 7 *March* 1986)

Abstract—A numerical investigation is made of laminar mixed convection of air in a vertical channel containing a partial rectangular blockage on one channel wall. The wall containing the blockage is assumed to be heated while the other wall is assumed to be either adiabatic (asymmetric heating) or heated (symmetric heating). Results indicate that at low values of Gr/Re^2 the maximum velocity occurs near the adiabatic wall in the asymmetrically heated channel. As Gr/Re^2 increases, this peak shifts towards the hot wall. Reverse flow is predicted beyond the blockage. In this reverse flow region temperature variations are small. The average Nusselt number in the blockage and the pre-blockage regions increases with decreasing Gr/Re^2 values. Beyond the blockage, the average Nusselt number decreases with Gr/Re^2 at high Rayleigh numbers. For the symmetrically heated channel, the velocity profiles are depressed at the center. For both thermal conditions (symmetric and asymmetric), the Nusselt numbers are smaller than the corresponding smooth duct Nusselt numbers.

INTRODUCTION

DURING the last decade, the trend in the electronic industry has been towards smaller computer components. This trend has been associated with increasing efforts for improved understanding of heat transfer cooling in electronic components. Typically, the simplest situations have received the primary attention. Natural convection in vertical heated channels has been studied extensively [1–6] to assess the magnitude of the self-induced cooling. Since fans are commonly employed in cooling electronic components, mixed convection in smooth ducts has also been studied [7–10].

Heat transfer correlations in smooth vertical ducts do not incorporate the effects of the finite disturbance introduced by the presence of the electronic components in the channel. So far, this effect does not appear to have received much attention in the literature. The objective of this paper is to study the heat transfer behavior of mixed convection in a partially blocked, vertical channel.

A schematic of the problem considered is shown in Fig. 1. The rectangular blockage on the right channel wall represents an electronic module on a vertical circuit board. Thus, the right wall is assumed to be at an elevated temperature T_h. Two thermal conditions are considered for the left wall. In one, the left wall is assumed to be adiabatic (representing a plate that does not contain any components). This defines the asymmetrically heated configuration. The other thermal condition corresponds to a heated left plate (that represents a plate containing electronic components on the exterior surface). This situation is referred to as the symmetrically heated configuration in this paper.

GOVERNING EQUATIONS AND SOLUTION PROCEDURE

The governing equations of the fluid are those that express the conservation of mass, momentum and energy. Because of the presence of the blockage, the flow is elliptic in nature. The flow is assumed to be steady, laminar and two-dimensional. These assumptions, for limited ranges of the governing parameter values, have been assumed in the literature to be valid for smooth ducts [7–9]. Radiation has been neglected in this study and therefore the results are applicable for moderate temperature differences.

The fluid is assumed to satisfy the Boussinesq approximation which relates the temperature to the

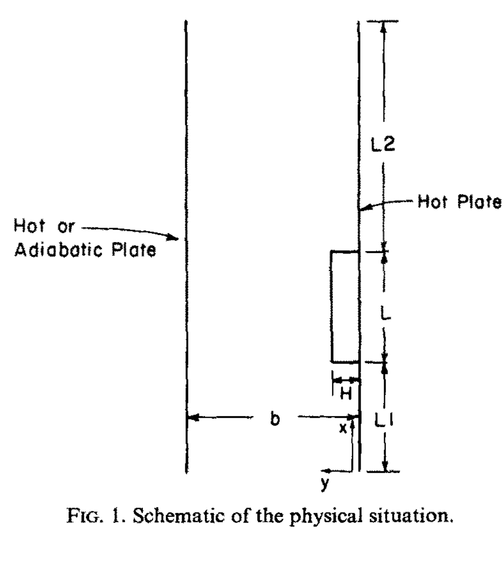

FIG. 1. Schematic of the physical situation.

NOMENCLATURE

b	channel width
c_p	specific heat at constant pressure
g	acceleration due to gravity
H	height of the blockage
k	thermal conductivity of fluid
$L, L1, L2$	length of the blockage, distance before the blockage, distance after the blockage
Nu_x, Nu_y	Nusselt number in the x and y directions
Nu	average Nusselt number
p, P	dimensional and dimensionless pressure
Pr	Prandtl number
Pe	Péclet number
Ra	Rayleigh number
Re	Reynolds number
T	temperature
T_h	temperature of hot surfaces
T_0	temperature of inlet air
U, V	dimensionless velocities
u, v	velocity components
u_0	dimensional inlet velocity
X	dimensionless coordinate, x/L
Y	dimensionless coordinate, y/L
x, y	coordinates.

Greek symbols

β	coefficient of thermal expansion
θ	dimensionless temperature
ν	kinematic viscosity
ρ	density
ρ_0	density of inlet air.

density through the following equation

$$\rho = \rho_0[1-\beta(T-T_0)] \tag{1}$$

where ρ_0 and T_0 are the corresponding density and temperature of the incoming flow. Also, a modified pressure is defined as follows

$$P^* = p+\rho_0 gx. \tag{2}$$

Using this definition and the Boussinesq approximation, the term $-\partial p/\partial x-\rho g$ in the x-momentum equation becomes $-\partial P^*/\partial x+\rho_0 g\beta(T-T_0)$.

The dimensionless variables chosen are

$$X = x/L, \quad Y = y/L, \quad U = u/u_0, \quad V = v/u_0 \tag{3a}$$

$$P = P^*/\rho u_0^2, \quad \theta = (T-T_0)/(T_h-T_0). \tag{3b}$$

The corresponding dimensionless governing equations are

$$\partial U/\partial X+\partial V/\partial Y = 0 \tag{4}$$

$$U\partial U/\partial X+V\partial U/\partial Y = -\partial P/\partial X+1/Re\cdot\nabla^2 U + Gr/Re^2\cdot\theta \tag{5}$$

$$U\partial V/\partial X+V\partial V/\partial Y = -\partial P/\partial Y+1/Re\cdot\nabla^2 V \tag{6}$$

$$U\partial\theta/\partial X+V\partial\theta/\partial Y = 1/Pe\cdot\nabla^2\theta \tag{7}$$

where

$$Gr = \rho g\beta(T_h-T_0)L^3/\nu^2, \quad Re = u_0 L/\nu,$$

$$Pr = \mu c_p/k, \qquad Pe = RePr. \tag{8}$$

The boundary conditions can be expressed as

at $X = 0$

$$U = 1, \quad V = 0, \quad \theta = 0 \tag{9}$$

at $Y = 0$

$$U = V = 0, \quad \theta = 1 \tag{10}$$

at $Y = b/L$

$$U = V = 0, \quad \theta = 1 \text{ or } \partial\theta/\partial Y = 0 \tag{11}$$

at $X = 1+(L1+L2)/L$

$$\partial U/\partial X = \partial V/\partial X = \partial\theta/\partial X = 0. \tag{12}$$

An examination of the dimensionless governing equations reveals three parameters: the Prandtl number (Pr), the Rayleigh number (Ra), and the Gr/Re^2 ratio. The Prandtl number is assigned the value of 0.7 corresponding to air. The Rayleigh number takes on values of 10^3, 10^5 and 10^6 while the Gr/Re^2 ratio is varied between 0.1 and 5.0.

In addition to the aforementioned parameters, there are four geometrical parameters: $L1/L$, $L2/L$, b/L and H/L. The parameters $L1/L$ and b/L have been assumed to be unity while the dimensionless blockage height H/L is assigned the values of 0.1 and 0.2. $L2/L$ is chosen to be sufficiently far downstream so that the zero streamwise gradient condition is satisfied.

The differential equations are solved using an implicit, elliptic finite difference procedure called SIMPLER (Semi Implicit Method for Pressure Linked Equations, Revised). This method has been developed by Patankar, and has been accorded a book length description in [11], and therefore, only a brief description is given here. In this method, the domain is subdivided into a number of control volumes, each associated with a grid point, and the governing differential equation is integrated over each control volume resulting in a system of algebraic equations that can be solved by an iterative technique. In the integration process, profile approximations are required in each coordinate direction and, for the results presented in this paper, an exponential profile approximation has been employed. Compared to the hybrid or the upwind profile approximations, the assumption of the exponential profile is associated with lower numerical diffusion and, is therefore, more accurate. To avoid checkerboard fields, the velocities are stored at staggered locations. The pressure–velocity linkage is resolved by a predictor–corrector technique.

To determine the appropriate grid size with which grid independent solutions can be obtained, the calculations were done on increasingly finer grid size distributions. A 56×46 non-uniform grid with a denser clustering near the walls was considered to give grid-independent results. To corroborate this, the 56×46 grid results were compared with the solution on an 80×80 non-uniform grid. The two results compare very well with each other with a maximum local difference of 4% in the two solutions. In addition, overall conservation of momentum and energy is satisfied to within 1% with the 56×46 grid.

RESULTS AND DISCUSSION

Results presented include streamline and isotherm patterns, dimensionless temperature and velocity profiles, and average and local Nusselt number distributions. In the discussion that follows, results are presented first for the asymmetrically heated channel followed by those of the symmetrically heated channel.

Asymmetrically heated channel (adiabatic left plate)

Streamline and isotherm patterns. Figures 2 and 3 show the streamline and the isotherm patterns for

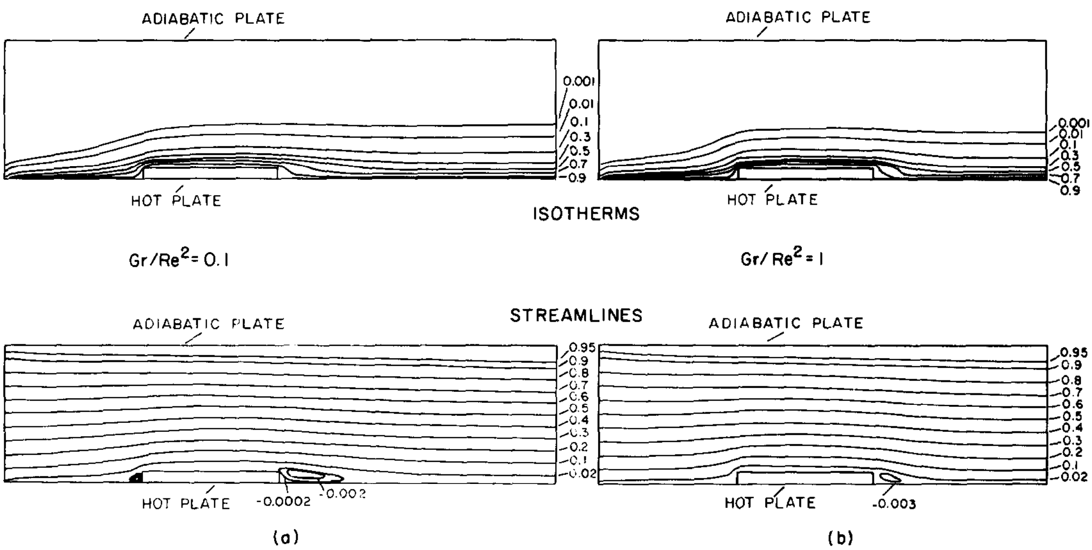

FIG. 2. Isotherms and streamlines for $Re = 1195$, $H/L = 0.1$: (a) $Gr/Re^2 = 0.1$; (b) $Gr/Re^2 = 1$.

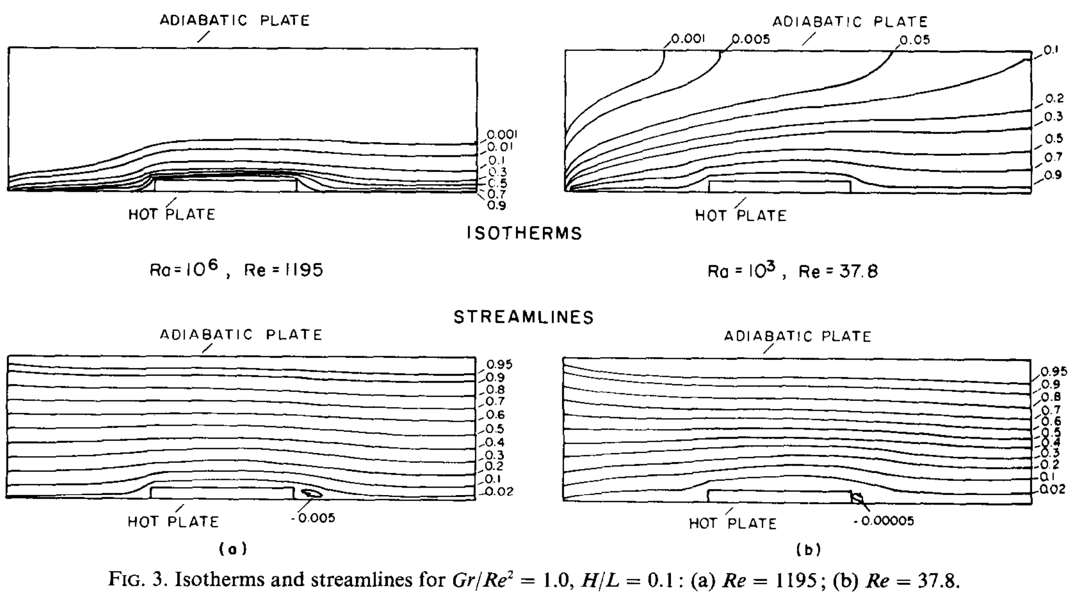

FIG. 3. Isotherms and streamlines for $Gr/Re^2 = 1.0$, $H/L = 0.1$: (a) $Re = 1195$; (b) $Re = 37.8$.

Table 1. Reattachment lengths

				x/L	
		Re	Gr/Re^2	Hot left plate	Adiabatic left plate
$Ra = 10^6$	$H/L = 0.2$	1195	1.0	2.54	2.65
		690.1	3.0	2.36	2.37
	$H/L = 0.1$	1195	1.0	2.28	2.33
		690.1	3.0	2.21	2.24
$Ra = 10^5$	$H/L = 0.2$	1195	0.1	3.60	3.60
		378	1.0	2.44	2.51
		218	3.0	2.30	2.35
		169	5.0	2.26	2.29
	$H/L = 0.1$	1195	0.1	2.58	2.57
		378	1.0	2.23	2.23
		218	3.0	2.17	2.19
		169	5.0	2.16	2.16
$Ra = 10^3$	$H/L = 0.2$	119.5	0.1	2.55	2.55
		37.8	1.0	2.25	2.25
		21.8	3.0	2.18	2.19
		16.9	5.0	2.175	2.175
	$H/L = 0.1$	119.5	0.1	2.18	2.20
		37.8	1.0	2.10	2.11
		21.8	3.0	2.09	2.09
		16.9	5.0	2.08	2.08

different parameter values. As the flow approaches the blockage, the streamlines are deflected towards the adiabatic wall and therefore, in the partially blocked region, the streamlines are more densely packed. Beyond the blockage ($x/L > 2.0$), the flow separates and reattaches further downstream on to the hot plate. The isotherm distribution expectedly shows a monotonic decrease of temperature from the hot wall to the adiabatic surface.

The influence of buoyancy (or Grashof number) can be observed in Fig. 2 which shows the streamline and isotherm patterns for $H/L = 0.1$, $Re = 1195$, and $Gr/Re^2 = 0.1$ and 1.0, respectively. For $Gr/Re^2 = 0.1$, a small eddy is observed near the leading edge of the blockage. As Gr/Re^2 increases to 1, this small leading edge eddy disappears while the recirculation region behind the blockage becomes smaller. This can also be seen in Table 1 where the reattachment lengths for the various cases considered are presented. This behavior is expected since, for large Gr/Re^2, the strong buoyant upflow along the vertical surface inhibits the size of the separated eddy. In view of the increasing eddy sizes as Gr/Re^2 values become smaller, the streamlines beyond the blockage are shifted towards the adiabatic wall as Gr/Re^2 is decreased.

The influence of the Reynolds number (at a constant Gr/Re^2) can be seen by comparing the different plots in Fig. 3. In view of the stronger motion at $Re = 1195$, the recirculating eddy is stronger and larger in Fig. 3(a) as compared to that in Fig. 3(b) ($Re = 37.8$). Furthermore, and as expected, the thermal boundary layer increases in thickness with decreasing Reynolds number. In fact, at $Re = 37.8$, no boundary-layer behavior is observed.

When the height of the blockage is decreased from 0.2 to 0.1, the size of the recirculating eddy decreases. The comparison of the reattachment length for the two blockage heights is shown in Table 1. Also, the thermal gradients near the hot wall are larger for $H/L = 0.1$. Although other quantitative differences exist, the qualitative behavior of the streamlines and the isotherms in both cases ($H/L = 0.1$, $H/L = 0.2$) are similar.

Temperature distribution. The temperature distribution across the channel is presented in Fig. 4 for different Gr/Re^2 values. At $x/L = 0.77$, the temperature distribution exhibits a boundary-layer behavior near the hot surface. As Gr/Re^2 is increased, the influence of natural convection becomes increasingly important. Since natural convection boundary layers are thicker compared to forced convection boundary layers, the temperature gradients at the wall are expectedly smaller and the temperature profile is more uniform at higher Gr/Re^2 values. Beyond the blockage ($x/L = 2.17$), the presence of the recirculating eddy distorts the temperature profile (Fig. 4). This distortion is explained by noting that as the flow moves backwards along the hot surface and towards the blockage, it transports energy towards the interior of the eddy and thus arrests the temperature decrease. Therefore, a decrease in the slope of the temperature profile is observed in the recirculating region. It may be noted that in the recirculating eddy, the dependence of the temperature profile on Gr/Re^2 is opposite to that

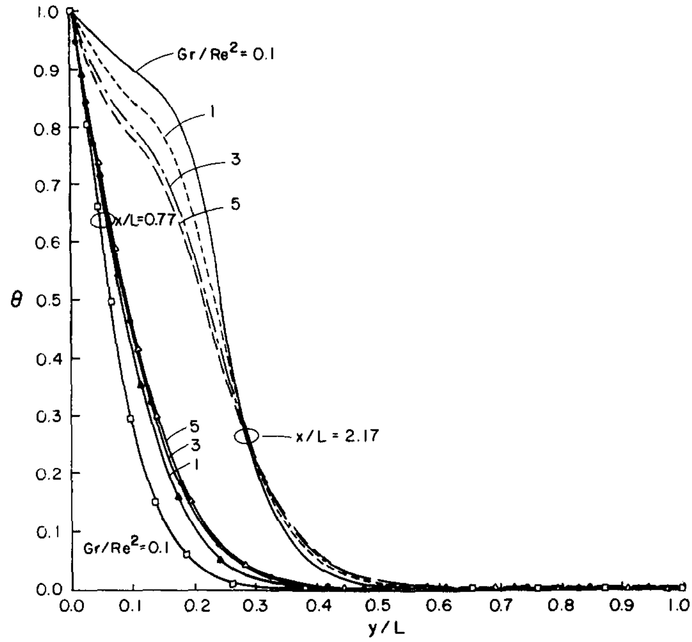

FIG. 4. Temperature distribution across the asymmetrically heated channel: $Re = 10^5$, $H/L = 0.2$.

observed outside the eddy, i.e. temperatures decrease with increasing Gr/Re^2. This trend reverses around $y/L = 0.25$.

Velocity distribution. The U-velocity profile across the channel for different Gr/Re^2 values is plotted in Fig. 5 for $Ra = 10^5$ and $H/L = 0.2$. At $x/L = 0.77$, the maximum velocity at $Gr/Re^2 = 0.1$ occurs near the adiabatic plate while at $Gr/Re^2 = 5.0$, the maximum velocity occurs near the hot plate. At low values of Gr/Re^2, the forced convection effects are dominant and the presence of the blockage causes the flow to be diverted towards the adiabatic wall resulting in a velocity maximum near the adiabatic plate. As Gr/Re^2 is increased, the natural convection effect becomes

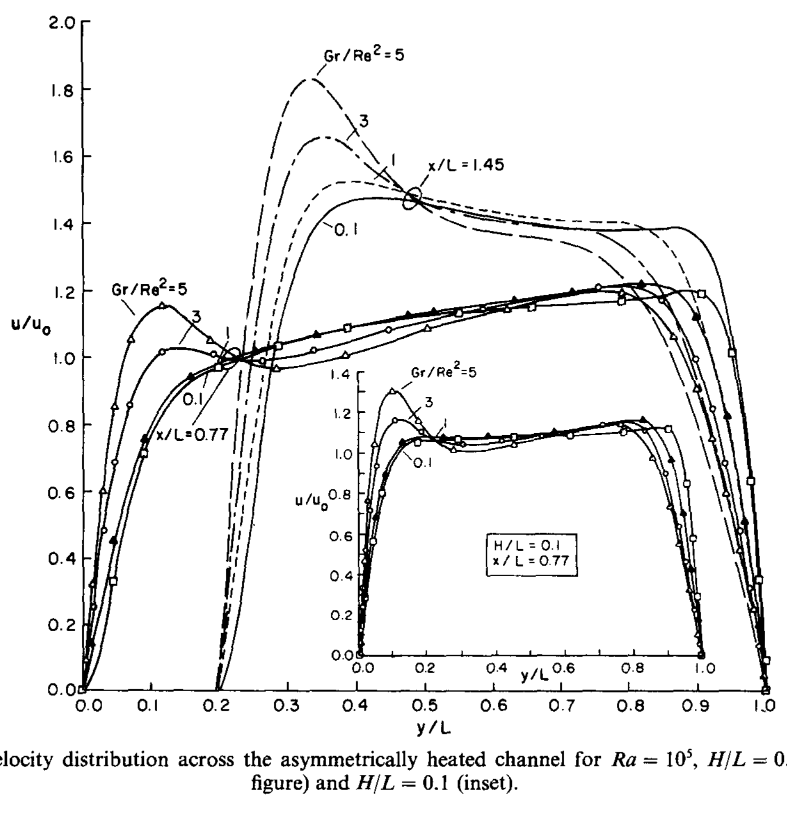

FIG. 5. Velocity distribution across the asymmetrically heated channel for $Ra = 10^5$, $H/L = 0.2$ (main figure) and $H/L = 0.1$ (inset).

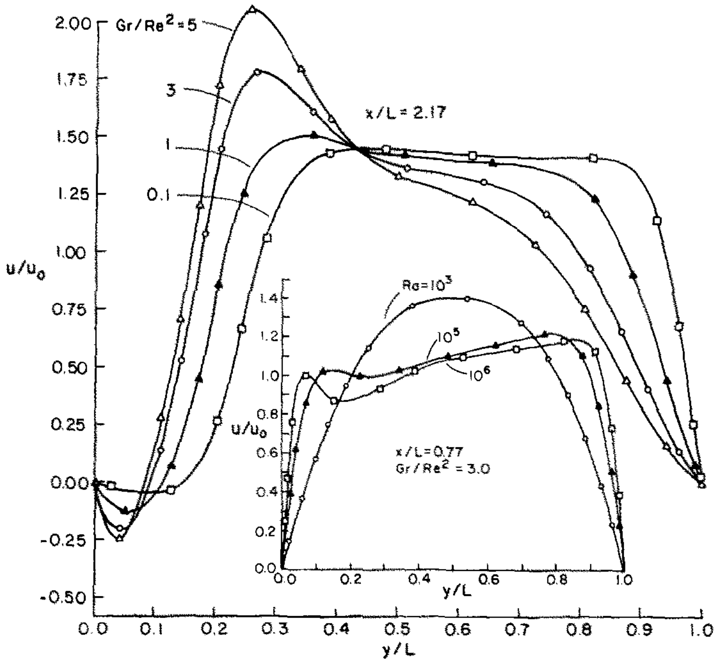

FIG. 6. Velocity distribution across the asymmetrically heated channel for different Gr/Re^2 values and Rayleigh numbers.

increasingly important and therefore, the peak velocity shifts closer to the hot surface. In the blockage region ($x/L = 1.45$) the velocity levels are generally higher due to the smaller flow area. At $x/L = 2.17$ (beyond the blockage), negative velocities are observed due to the recirculating eddy (Fig. 6). The magnitude of the negative velocity increases as Gr/Re^2 increases. However, as noted earlier, the recirculation region is smaller at higher Gr/Re^2 values.

If the blockage height is decreased from 0.2 to 0.1, the qualitative behavior of the velocity profiles remains the same. However, there are quantitative differences. The inset of Fig. 5 presents the U-velocity profiles at $x/L = 0.77$ for $H/L = 0.1$. As H/L decreases, the boundary-layer behavior near the hot surface becomes more pronounced.

The effect of changing the Rayleigh number and Reynolds number, and keeping Gr/Re^2 constant is shown in the inset of Fig. 6. As the Rayleigh number is increased, velocity boundary layers develop near the hot side of the channel. At $Ra = 10^3$, the natural convection effects are small and the velocity profile is almost symmetrical. At $Ra = 10^6$, the effects of buoyancy and the presence of the blockage result in local peaks near the two walls with a depression in-between.

Nusselt numbers. To present the heat transfer data, the Nusselt number is calculated along the heated surfaces using the following definition.

$$Nu_x = hL/k \tag{13}$$

where

$$h = -k \cdot \partial T/\partial y|_{y=0}/(T_h - T_0) \tag{14}$$

is the heat transfer coefficient based on the wall to the inlet temperature difference.

Local Nusselt number. Plots for the local Nusselt numbers (Nu_x) along the hot plate and the blockage surface parallel to it are presented in Fig. 7. In general, the Nusselt number values decrease with Rayleigh number. The Nusselt number attains a maximum value near the channel inlet and decreases as x/L increases towards the blockage. This is expected because the surface near the entrance is washed by the cold fluid (zero dimensionless temperature). As the fluid flows along the hot surface, its temperature increases and the heat transfer coefficient correspondingly decreases. Along the vertical surface of the blockage (parallel to the x-axis) the same behavior is observed. Beyond the blockage, the Nusselt number behavior is noticeably different due to the recirculating eddy in that region. The Nusselt number increases up to the point of reattachment and then decreases gradually towards the exit of the channel. At the point of reattachment, the heat flux and therefore, the Nusselt number values peak. On either side of this point of reattachment, the flow is directed outwards and, therefore, the Nusselt number (Nu_x) values expectedly decrease. For $Ra = 10^3$, the recirculation eddy is very small and weak. Therefore, unlike the other Rayleigh numbers, a monotonic increase towards the channel exit is observed.

The influence of Gr/Re^2 should also be noted. For the higher Rayleigh numbers, as Gr/Re^2 increases, the strength of the recirculating eddy increases leading to higher Nu_x values (Fig. 7). Since the size of the eddy is reduced at higher Gr/Re^2, Nu_x peaks at a smaller x/L

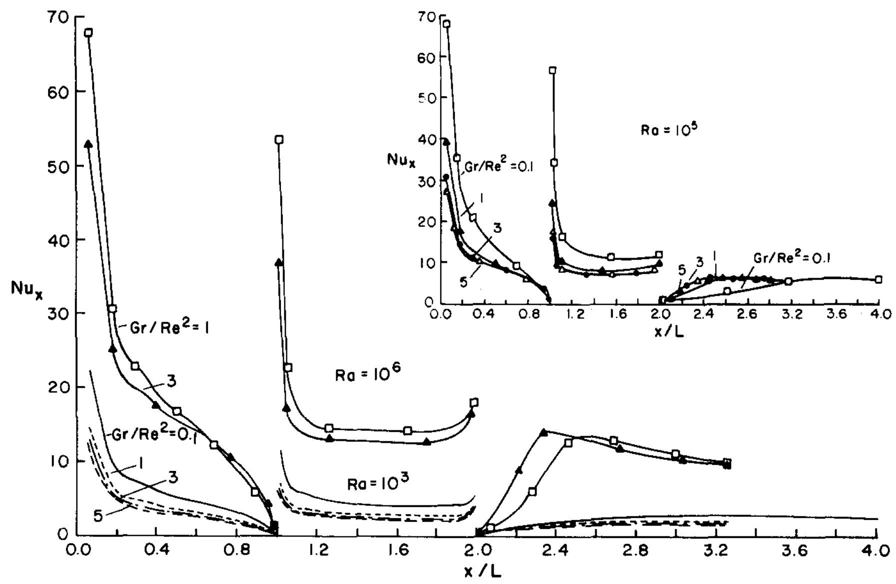

FIG. 7. Nusselt number distribution along the hot wall for the unsymmetrically heated channel, $H/L = 0.2$.

value. Between $x/L = 0$ and $x/L = 2$, Nu_x decreases as Gr/Re^2 increases. This is because the temperature profiles are more uniform at higher Gr/Re^2 values resulting in lower heat transfer coefficients.

The Nusselt number along the horizontal surfaces of the blockage (Nu_y) is presented in Fig. 8. It should be noted that Nu_y at $x/L = 1$ (inset of Fig. 8), is of the same order of magnitude as Nu_x while Nu_y at $x/L = 2$ is much smaller than Nu_y at $x/L = 1$ due, in part, to the fluid being warmer at $x/L = 2$ and therefore less amenable to heat transfer.

At a higher Rayleigh number, Nu_y along the upper surface of the blockage increases as Gr/Re^2 increases (Fig. 8), due to the increase in the recirculating eddy strength with Gr/Re^2. At the lower Rayleigh number ($Ra = 10^3$), the recirculating eddy beyond the blockage is very small and weak and the values of Nu_y decrease as Gr/Re^2 increases.

Average Nusselt number. The average Nusselt number along a length Δs is defined as

$$\overline{Nu} = \frac{1}{\Delta s}\int_s^{s+\Delta s} Nu(s)\,\mathrm{d}s \tag{15}$$

where s represents either x or y. The average Nusselt number along the vertical surfaces and along the

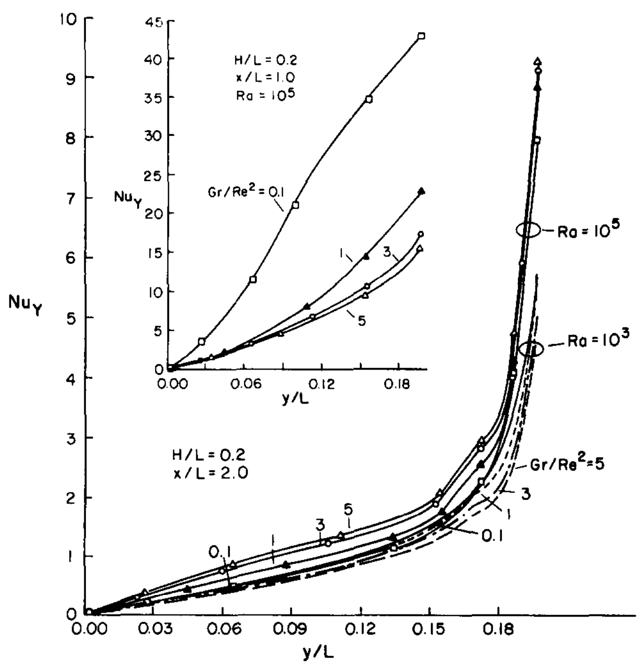

FIG. 8. Local Nusselt number along the lower ($x/L = 1.0$) and upper ($x/L = 2.0$) surface of the blockage.

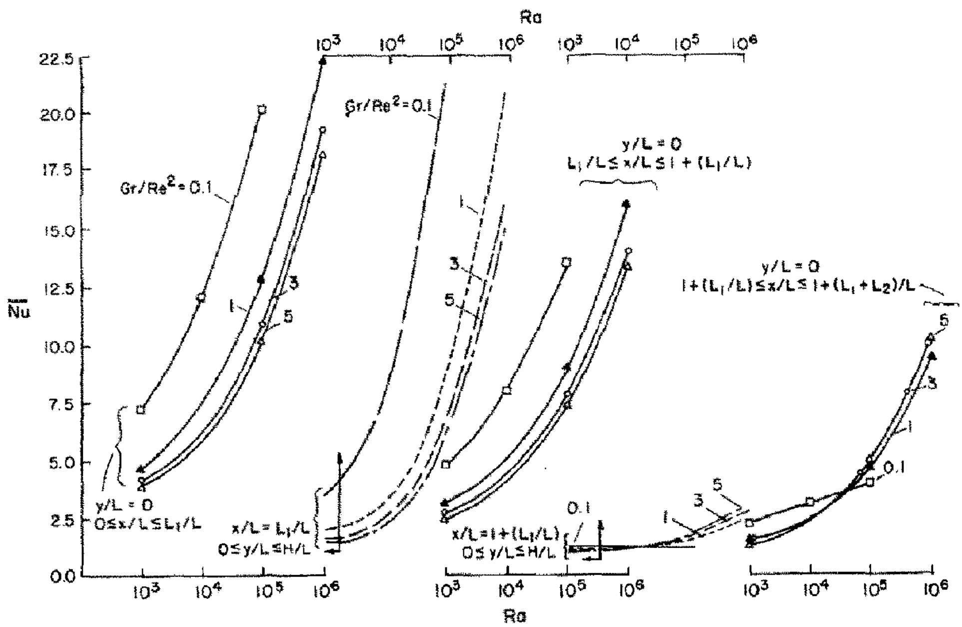

FIG. 9. Average Nusselt number distributions along the vertical surfaces (solid lines) and along the horizontal surfaces of the blockage (dotted lines), $H/L = 0.2$.

upper and lower surfaces of the blockage are presented in Fig. 9 for $H/L = 0.2$. With increasing Rayleigh number, the strength of the flow field and, therefore, the average Nusselt number, along the vertical surfaces increases. Between $x/L = 0$ and $x/L = 2$, the average Nusselt number increases as Gr/Re^2 decreases. However, above the blockage ($x/L > 2$) and at high Rayleigh numbers, the average Nusselt number increases with increasing Gr/Re^2. To explain this, it should be noted that at the high Rayleigh numbers, as Gr/Re^2 decreases the size of the recirculation beyond the blockage increases (Fig. 2) and, since the recirculation region is associated with low heat transfer rates, the average heat transfer or Nusselt number from the plate is therefore expected to decrease with decreasing Gr/Re^2. At low Ra and Re, the recirculation zone is very small and its effects are not significant. Hence, the Nu trends follow those along $0 \leqslant x/L \leqslant 2$, i.e. decreasing Nu with increasing Gr/Re^2.

The average Nusselt number along the upper and lower surfaces of the blockage is shown by dotted lines in Fig. 9. At the lower surface ($x/L = 1$), the average Nusselt number increases with increasing Rayleigh number and decreasing Gr/Re^2. On the other hand, at the upper surface ($x/L = 2$), the dependence of the average Nusselt number on Gr/Re^2 reverses at higher Rayleigh numbers due to the effect of recirculating eddy beyond the blockage.

Table 2 shows the overall average Nusselt number values for a blocked vertical channel ($H/L = 0.2$) and a smooth vertical channel ($H/L = 0$) at $Ra = 10^3$. Results for the smooth channel were obtained using a parabolic finite-difference procedure of Patankar and Spalding [12]. It is noted that the average Nusselt number values are higher for the smooth channel. This result is somewhat unexpected and is due, in part, to the near-isothermal recirculation region behind the blockage which, as noted earlier, is characterized by low heat transfer rates.

Symmetrically heated channel (heated left plate)

In describing the results for the symmetrically heated channel, the discussion is limited primarily to the observed similarities and differences with the results of the asymmetrically heated channel.

Temperature distribution. The temperature profiles across the channel for $Ra = 10^5$, $H/L = 0.2$, and the various Gr/Re^2 values are shown in Fig. 10. At $x/L = 0.77$, it is observed that the temperature exhibits a boundary-layer behavior near both plates. However, the temperature values are generally higher near $y/L = 0$, due to the higher heat transfer area. Beyond the blockage (at $x/L = 2.17$), the temperature profile is distorted, as for the asymmetrically heated channel, due to the recirculating eddy.

Velocity distribution. The U-velocity profiles across the channel are presented in Fig. 11 for $Ra = 10^5$, $H/L = 0.2$, and the various Gr/Re^2 values. At $x/L = 0.77$, it is observed that the velocity peaks near both plates with the maximum occurring near the left

Table 2. Overall average Nusselt number, $Ra = 10^3$

$Gr/Re^2 =$	0.1	1.0	3.0	5.0
Smooth channel ($H/L = 0$)	4.4521	3.6219	3.4590	3.4512
Blocked channel ($H/L = 0.2$)	4.4062	3.5709	3.3936	3.3621

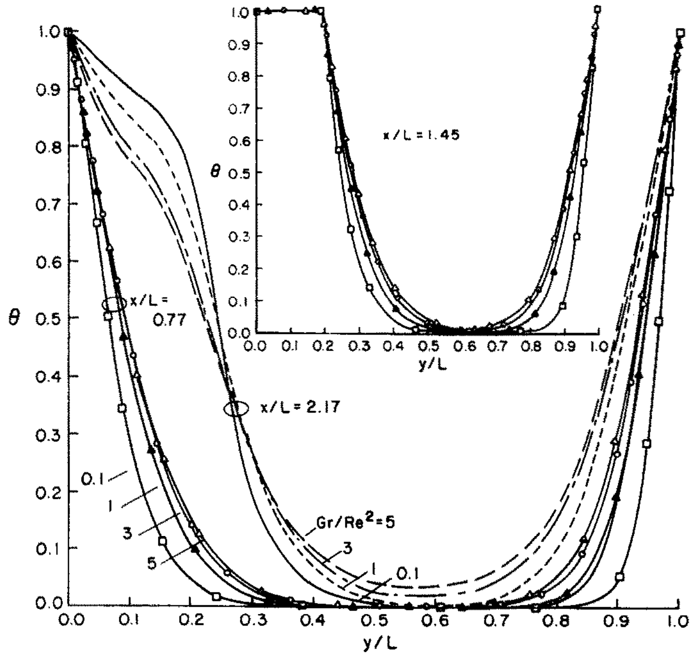

FIG. 10. Temperature distribution in the symmetrically heated channel.

plate ($y/L = 1.0$). The presence of the blockage causes the flow to be deflected towards the left plate causing the velocity to attain its maximum in that region. With increasing x/L the velocity near both walls increase and since the channel flow rate is constant, this results in a concavity in the profile in the center. The magnitude of this concavity increases as the flow moves downstream as seen in the inset of Fig. 12 ($x/L = 2.17$). This significant depression in the velocity profile is not observed in the asymmetrically heated channel. Negative velocities are once again observed (Fig. 12) beyond the blockage due to the recirculating eddy.

The effect of the Rayleigh number can be seen in Fig. 12. As expected, at a high Rayleigh number ($Ra = 10^6$), natural convection effects near the wall are dominant and a large depression in the velocity profile is observed around the center line. On the other hand, at a low Rayleigh number ($Ra = 10^3$), the

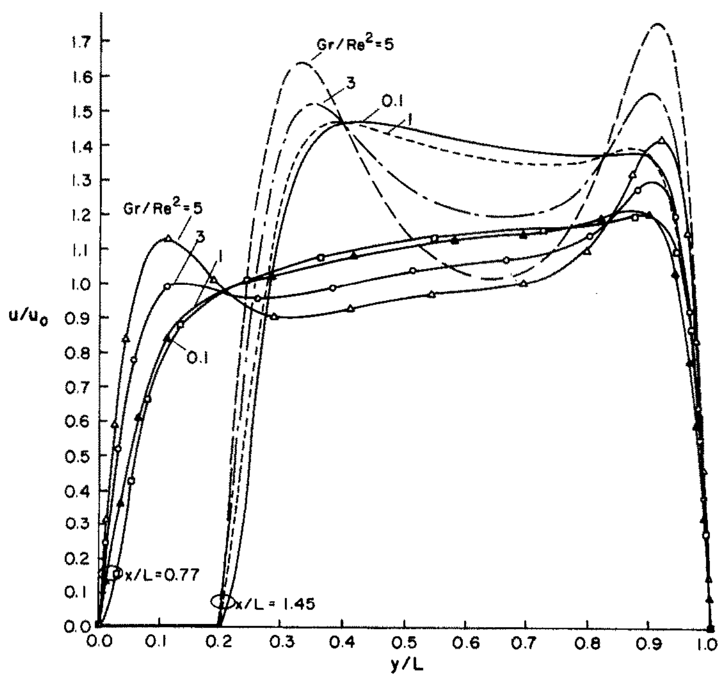

FIG. 11. Velocity distribution across the symmetrically heated channel, $Ra = 10^5$.

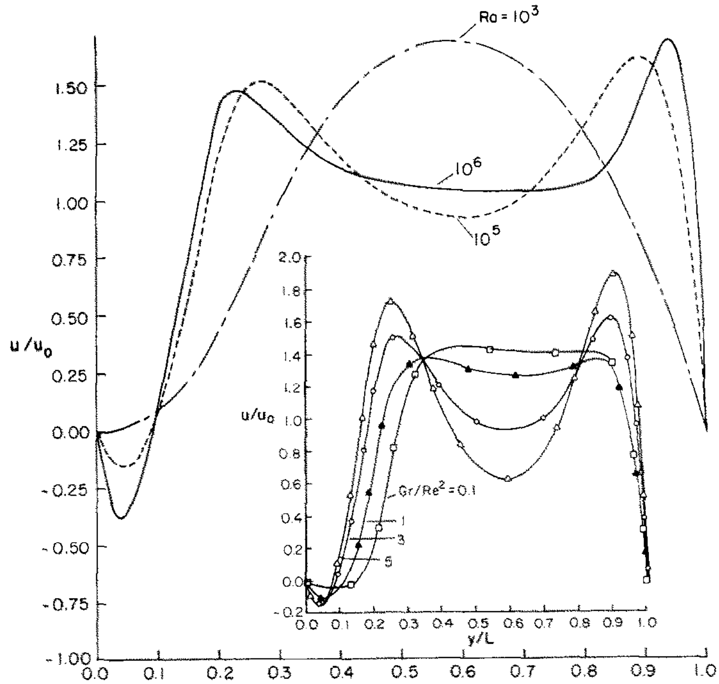

FIG. 12. Velocity distribution across the symmetrically heated channel at $x/L = 2.17$.

velocity profile is more uniform and no concavity is observed.

Nusselt numbers. The general behavior, as well as the effect of the governing parameters on the local Nusselt number distribution along the right side of the channel are the same as observed in the asymmetrically heated channel, but the magnitudes of Nu_x are lower by about 10%. The local Nusselt number profiles along the left plate of the heated channel are presented in Fig. 13 for $H/L = 0.2$. Expectedly, the local Nusselt number attains a maximum value near the entrance of the channel and decreases as the flow approaches the exit. As Gr/Re^2 increases, the Nusselt numbers decrease. The inset of Fig. 13 shows the local Nusselt number along the left plate for both the blocked channel ($H/L = 0.2$) and the smooth channel ($H/L = 0$). As for the asymmetrically heated channel, the values of Nu_x are higher for the smooth channel.

Figure 14 shows that the average Nusselt number along the right plate is slightly lower for the symmetrically heated channel case. This is expected because the thermal boundary layer along the left

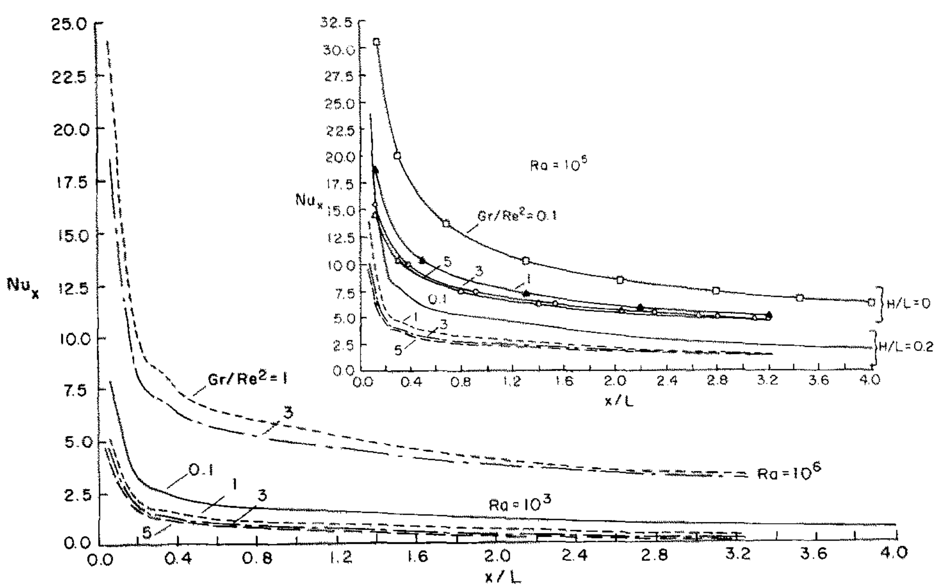

FIG. 13. Nusselt number distribution along the smooth plate of the symmetrically heated channel.

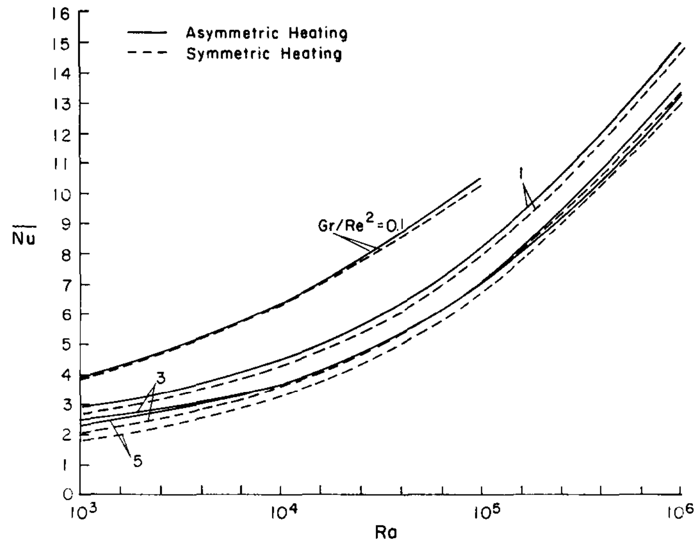

FIG. 14. Overall average Nusselt number along the hot wall containing the blockage ($H/L = 0.2$).

plate, causes the core temperature to increase which results in lower temperature gradients along the right plate boundary layer which reduces the heat transfer.

CONCLUDING REMARKS

Mixed convection in a partially blocked, vertical channel has been investigated by a numerical procedure. As Gr/Re^2 increases, the recirculation region above the blockage becomes stronger and smaller. In the recirculation region the temperature profile exhibits a smaller rate of decrease. The local and average Nusselt numbers increase with decreasing Gr/Re^2 in the blockage and the pre-blockage areas while, in the recirculation region, the local and average Nusselt numbers increase with Gr/Re^2 at high Rayleigh numbers. A local maximum in the Nusselt number distribution is obtained at the point where the separated flow beyond the blockage reattaches. The average Nusselt number along the lower horizontal surface of the blockage is comparable to the Nusselt numbers along the vertical walls but significantly larger than the Nusselt number along the upper horizontal face of the blockage. Decreasing the dimensionless blockage thickness from 0.2 to 0.1 does not change the qualitative behavior although quantitative differences are noted. For the symmetrically heated channels, the velocity profiles are depressed in the center and become increasingly depressed as Gr/Re^2 increases. For both symmetric and asymmetric heating cases, the Nusselt numbers are smaller than the corresponding smooth duct Nusselt numbers.

REFERENCES

1. J. R. Bodia and J. F. Osterle, The development of free convection between heated vertical plates, *J. Heat Transfer* **84C**, 40–44 (1962).
2. W. Elenbass, Heat dissipation of parallel plates by free convection, *Physica* **9**, 1–28 (1942).
3. W. Aung, Fully developed laminar free convection between vertical parallel plates heated asymmetrically, *Int. J. Heat Mass Transfer* **15**, 1577–1580 (1972).
4. H. Nakamura, Y. Asoko and T. Naitou, Heat transfer by free convection between two parallel flat plates, *Numer. Heat Transfer* **5**, 39–58 (1982).
5. W. Aung, L. S. Fletcher and V. Sernas, Developing laminar free convection between vertical flat plates with asymmetric heating, *Int. J. Heat Mass Transfer* **15**, 2293–2308 (1972).
6. C. F. Kettleborough, Transient laminar free convection between heated vertical plates including entrance effects, *Int. J. Heat Mass Transfer* **15**, 883–896 (1972).
7. S. Ostrach, Combined natural and forced convection laminar flow and heat transfer of fluid with and without heat sources in channels with linearly varying wall temperature, NACA TN, 3141 (1954).
8. T. Cebeci, A. A. Khattab and R. Lemont, Combined natural and forced convection in vertical ducts, *Proc. Seventh Int. Heat Transfer Conference*, Munich, F.R.G., Vol. 1 (1982).
9. A. M. Dalbert, Natural, mixed and forced convection in a vertical channel with asymmetric uniform heating, *Proc. Seventh Int. Heat Transfer Conference*, Munich, F.R.G., Vol. 1 (1982).
10. J. Quintiere and W. K. Muller, An analysis of laminar free and forced convection between parallel plates, *J. Heat Transfer* **95**, 53–59 (1973).
11. S. V. Patankar, *Numerical Heat Transfer and Fluid Flow*. Hemisphere, New York (1980).
12. S. V. Patankar and D. B. Spalding, *Heat and Mass Transfer in Boundary Layers*. Intertext, London (1970).

CONVECTION MIXTE LAMINAIRE DANS UN CANAL VERTICAL PARTIELLEMENT BLOQUE

Résumé—On étudie numériquement la convection mixte laminaire d'air dans un canal vertical contenant un blocage partiel rectangulaire sur une paroi d'un canal; cette paroi est supposée chauffée tandis que l'autre est soit adiabatique (chauffage asymétrique) ou chauffée (chauffage symétrique). Les résultats indiquent qu'aux faibles valeurs de Gr/Re^2, le maximum de vitesse se produit près de la paroi adiabatique dans le cas de chauffage asymétrique. Lorsque Gr/Re^2 augmente ce pic se déplace vers la paroi chaude. Un écoulement de retour est derrière le blocage. Dans cette région les variations de température sont petites. Les nombres de Nusselt moyen dans le blocage et avant le blocage augmentent quand diminue Gr/Re^2. Au-dessus du blocage, le nombre de Nusselt moyen diminue avec Gr/Re^2 aux grands nombres de Rayleigh. Pour le canal chauffé symétriquement, les profils de vitesse sont déprimés au centre. Pour les deux conditions thermiques (symétrique et asymétrique), les nombres de Nusselt sont plus petits que ceux relatifs au canal lisse correspondant.

LAMINARE GEMISCHTE KONVEKTION IN EINEM TEILWEISE VERSPERRTEN VERTIKALEN KANAL

Zusammenfassung—Es wurde eine numerische Untersuchung der laminaren gemischten Konvektion von Luft in einem vertikalen Kanal, der durch ein rechteckiges Hindernis auf einer Kanalwand teilweise versperrt ist, durchgeführt. Es wurde angenommen, daß die Wand mit dem Hindernis beheizt wird, während die andere Wand entweder adiabat (asymmetrische Beheizung) oder beheizt (symmetrische Beheizung) sein soll. Die Ergebnisse zeigen, daß für kleine Werte von Gr/Re^2 die maximale Geschwindigkeit im asymmetrisch beheizten Kanal nahe der adiabaten Wand auftritt. Für zunehmende Gr/Re^2-Werte verschiebt sich das Maximum in Richtung auf die heiße Wand. Jenseits des Hindernisses ergibt sich eine Umkehrung der Strömung. In dem Gebiet der Rückwärtsströmung sind die Temperaturunterschiede sehr gering. Die mittlere Nusselt-Zahl in den Gebieten vor und innerhalb des Hindernisses steigt mit abnehmenden Gr/Re^2-Werten. Jenseits des Hindernisses nimmt die mittlere Nusselt-Zahl mit Gr/Re^2 für große Rayleigh-Zahlen ab. Beim symmetrisch beheizten Kanal sind die Geschwindigkeitsprofile in der Mitte abgeflacht. Für beide thermischen Bedingungen (symmetrisch und asymmetrisch) sind die Nusselt-Zahlen kleiner als die für einen entsprechenden glatten Kanal.

ЛАМИНАРНАЯ СМЕШАННАЯ КОНВЕКЦИЯ В ЧАСТИЧНО ЗАГРОМОЖДЕННОМ ВЕРТИКАЛЬНОМ КАНАЛЕ

Аннотация—Проведено численное исследование ламинарной смешанной конвекции воздуха в вертикальном канале, к одной стенке которого прикреплены прямоугольные перегородки. Предполагается, что стенка с перегородками нагревается, в то время как другая считается либо адиабатической (асимметричный нагрев), либо нагретой (симметричный нагрев). Результаты показывают, что при малых значениях Gr/Pe^2 максимум скорости имеет место вблизи адиабатической стенки асимметрично нагреваемого канала. С увеличением Gr/Pe^2 этот максимум смещается в направлении горячей стенки. Предсказано существование обратного течения за перегородкой. В зоне обратного течения изменения температуры малы. Среднее число Нуссельта на перегородке и в зонах перед ней растет с уменьшением значений Gr/Pe^2. За перегородкой среднее число Нуссельта уменьшается с Gr/Pe^2 при больших числах Рэлея. Для случая симметричного нагреваемого канала профили скорости сжимаются в центре. Для обоих тепловых режимов (симметричного и несимметричного) числа Нуссельта меньше соответствующих чисел для гладкого канала.